Vibrational Relaxation Dynamics of Azide in Ionic and Nonionic Reverse Micelles

Gerald M. Sando,[†] Kevin Dahl,[‡] and Jeffrey C. Owrutsky*

Code 6111, U.S. Naval Research Laboratory, Washington, D.C. 20375-5342

Received: August 13, 2004; In Final Form: October 10, 2004

Ultrafast infrared spectroscopy has been used to measure vibrational energy relaxation (VER) and reorientation times (T_r) for the antisymmetric stretching band of azide ion (N_3^-) in several reverse micelle (RM) systems using cationic, anionic, and nonionic surfactants. RMs were formed using H_2O for all surfactants and D_2O for the anionic and cationic surfactants. The vibrational dynamics depended on the RM charge. The charge dependence is attributed to differences in ion location in the RM because of Coulombic interactions. The VER times in anionic (AOT, sodium bis(2-ethylhexyl) sulfosuccinate) RMs are indistinguishable from those in bulk solution and T_r times are longer only for the smallest RMs studied. In cationic (CTAB, cetyltrimethylammonium bromide) RMs, VER and T_r times are longer and weakly depend on the RM water content and water pool size. The results are attributed to the azide anion being attracted toward the RM wall when it is cationic and repelled into the bulklike center when it is anionic. VER times are also longer in small nonionic RMs (NP and Brij-30) but, unlike cationic RMs, approach bulk behavior as the RM size is increased. Comparative studies are performed using mixtures of water and tri(ethylene glycol) monomethyl ether (TGE) in which the latter resembles the hydrophilic portion of the nonionic surfactants. The similar results for nonionic RMs and TGE/water mixtures provide evidence that water penetrates into and hydrates the poly-oxo chains in the nonionic RMs before a water pool is formed. The interfacial region in nonionic RMs include the poly-oxo chains, which appear to be hydrated, so that the boundary between the interface and the water core is less clearly defined than for the ionic RMs.

Introduction

The properties of molecules are often affected when they are confined to regions with dimensions of a few molecular diameters. Confined water in particular has received a great deal of attention because of its relevance to biological systems.[1−3] Nanoconfined aqueous systems have been studied in nanoporous glasses as well as in cyclodextrin cavities.[4−9] Another easily controlled method of nanoconfinement, albeit with a softer interface, is the use of reversed micellar systems. Reverse micelles (RMs) are nanosized water droplets formed in bulk organic solvent that are stabilized by the presence of surfactants. A convenient property of RMs is that they are relatively monodisperse and the water pool size can be controlled because of its monotonic dependence on water content. The water content is often characterized by the molar ratio of water to surfactant, ω, where $\omega = [H_2O]/[\text{surfacant}]$. RM water pool sizes are generally on the order of tens of angstroms with radii that vary linearly with ω and have been characterized for a variety of surfactants using dynamic light scattering, fluorescence quenching, and small-angle X-ray and neutron scattering techniques.[10−19] Various spectroscopic studies have provided an overall picture of the aqueous environment inside of a RM that is different than bulk water. The extent of hydrogen bonding is reduced, as evidenced by a blueshift of the O−H stretching IR bands of water.[20−23] The water pool is also less polar, as evidenced by reduced solvatochomatic shifts of solutes compared to those in bulk water.[24,25] Experimental[20−23,26,27] and modeling[28−32] studies suggest a layered water pool structure in which there are water molecules hydrating the surfactant headgroups,[33] possibly an intermediate layer consisting of the next few nearest neighbors, and for large enough RMs, a bulklike interior region.

Previous time-resolved studies have revealed longer time constants for dynamical processes in RMs than for bulk water. These studies have included solvation dynamics,[34−45] internal charge transfer,[45−48] isomerization,[49,50] dielectric relaxation,[51,52] and transient infrared spectroscopy.[53−56] RMs can be formed using cationic, anionic, or nonionic surfactants. The spectral shifts and dynamics of solute probe species in RMs have been observed to depend on the surfactant charge, which is often related to the location of the probe within the RM. This has been shown in studies of solvation dynamics where both static spectral shifts and the time scales of solvation dynamics showed little dependence on ω for systems with oppositely charged probe and surfactant.[34] Larger dependences on ω were observed for nonionic surfactants and surfactant with the same charge as the probe.[37] When oppositely charged, the Coulombic attraction between the surfactant and the probe resulted in the probe residing in the interfacial region, an environment that changes little with ω. Time-resolved emission studies of $[Ru(bpy)_3]^{2+}$ showed a dependence on surfactant charge.[57] When a cationic surfactant was used, Coulombic repulsion actually caused a redistribution of RM sizes and biexponential behavior at small ω. For an anionic surfacant, the $[Ru(bpy)_3]^{2+}$ probe resided at the interface and showed monoexponetial behavior for all values of ω, again with little ω dependence. Similar behavior has been seen for fluorescence quenching of $Ru(bpy)_3^{2+}$ derivatives, where quenching rates were nearly independent of ω when the probe and surfactant were oppositely charged, but significant

* To whom correspondence should be addressed. E-mail: jeff.owrutsky@nrl.navy.mil.
† NRL-ASEE Research Associate.
‡ NRL-NRC Research Associate.

10.1021/jp0463363 CCC: $27.50
Published on Web 11/24/2004

ω dependences were seen when surfactant and probe have the same charge.[58] For hydrophobic probes, static spectral shifts[27] and solvation dynamics[44] are often independent of ω regardless of surfactant charge because the hydrophobic probes prefer the interface.

Since dynamics can depend sensitively on probe species location within the RM, it is important to determine where the probe is located when interpreting the results of dynamics measurements. Faeder and Ladanyi have performed molecular dynamics simulations of I_2^- in an anionic RM that predict the anionic solute to reside in the center of the water pool formed by the anionic surfactant.[30] In general, small ions are expected to be very hydrophilic and should prefer the center of the water pool in the absence of strongly attractive Coulombic forces. Recently, we have reported on the FTIR spectra of the antisymmetric stretch of azide (N_3^-) in RMs with cationic, nonionic, and anionic surfactants.[19] The IR band peak position depends on the surfactant charge, with the overall trend in frequency: CTAB (cationic cetyltrimethylammonium bromide) < NP (nonionic) < bulk H_2O < AOT (anionic sodium bis(2-ethylhexyl) sulfosuccinate). This trend agrees with the surfactant−solute Coulombic interaction in which a larger red shift is observed for more attractive positive surface charge. Unfortunately, the location of a solute within a RM is hard to determine unambiguously, so that it is difficult to ascertain whether the variations with surfactant charge for the IR spectra are due to solvation properties for ions in the water core or to solute−interface interactions.

We recently reported vibrational energy relaxation studies of azide ion, N_3^-, in nonionic RMs using the surfactant NP.[55,56] Azide is a benchmark small anion for fast VER. The antisymmetric stretching vibrational band has a large transition moment so that low concentrations of azide can be easily detected. The small ion is highly hydrophilic and therefore an ideal probe for studying confinement effects on ion solvation properties in the water pool of a RM. Azide is much smaller and more hydrophilic than many organic dyes that have been used to study RMs, decreasing the chances of perturbing the RM structure[57] and increasing the chances of locating a solute in the water pool rather than in the interfacial region as often occurs for organic dyes.[27,44,59] In addition, in bulk solutions the static spectral shift scales with the solvent polarity and correlates with the T_1 time for vibrational relaxation.[60,61] This provides a clear route to exploring confinement effects on local interactions as revealed by static and dynamic IR spectroscopy. VER dynamics studies of azide ion in the nonionic surfactant NP revealed VER rates that were slower than in the bulk by a factor of 3 for the smallest RMs and approached the bulk value as the RM size increased without reaching the bulk value.[56] Since the VER rate depends on the solute−solvent interaction strength, the longer T_1 times are consistent with the generally accepted idea of lower polarity and reduced hydrogen bonding in RM water pools. Our studies also included reorientation time measurements for small ions which demonstrated that T_r increased more than T_1 times.[55] The longer reorientation times reinforce the notion of reduced mobility in the RM interior.

In this work, IR pump/probe studies of azide in RMs are extended to ionic surfactants, including cationic CTAB and anionic AOT, as well as to a nonionic surfactant, Brij-30, with fewer hydrophilic poly-oxo units (4) than NP (7). Studies are performed in both H_2O and D_2O RMs for the ionic surfactants. In the absence of deuterated surfactants, measurements in D_2O are precluded because of isotopic contamination for the nonionic surfactants that have alcoholic headgroups with labile hydrogens. The longer VER lifetimes in D_2O extend the time scale for anisotropy measurements and facilitate determination of the reorientation times. Our previous FTIR studies revealed a frequency shift at small ω that depended on surfactant charge.[19] We offered several possible explanations including ion location and, for AOT, counterion effects. The present work, combined with the previous studies in nonionic NP RMs and in bulk solution, is intended to more clearly identify the location of the azide ion in the RM cavity and how surfactant charge influences confinement effects of ions in RMs. In addition, dynamics are measured in bulk mixtures of H_2O and tri(ethylene glycol) monomethyl ether (TGE), which has a poly-oxo chain similar to the nonionic surfactants but without the hydrophilic portion, meant to simulate the interior of the nonionic RMs. Comparing the TGE/water mixtures (binary) to the RMs (ternary system) allows assessment of whether the ion resides in the water core.

Experimental Section

Details of the laser system can be found in our previous publication.[56] Briefly, the laser system consists of a titanium sapphire oscillator (Clark-MXR, Inc. NJA-5) pumped by a CW Nd:VO_4 laser (Spectra-Physics Millennia V). The oscillator output is amplified in a regenerative amplifier (Positive Light Spitfire) pumped by an Nd:YLF (Positive Light Merlin) providing ~100 fs pulses with an energy of ~900 μJ at 1 kHz near 800 nm. The amplified output pumps an optical parametric amplifier (TOPAS-4/800-FS, Light Conversion) generating 150 μJ of signal (1150−1600 nm) and idler (1600−2700 nm). Mid-IR pulses (2.4−11 μm) are generated by difference frequency mixing of the signal and idler pulses in a Type I $AgGaS_2$ crystal (2 mm) after traveling through a quartz time-plate. This provides IR pulses of ~4 μJ and 200 fs at 5 μm. The mid-IR beam is split into pump and probe (10%) components. The probe beam is directed to a translation stage and the pump beam is directed to a chopper operating at 500 Hz. The pump and probe are crossed at a small angle with the pump beam at the static sample cell after passing through a 75-mm CaF_2 lens. The probe beam polarization is controlled via a wire grid polarizer after the sample. The probe beam is sent to a monochromator with ~5 cm^{-1} resolution and detected with an HgCdTe infrared detector. The signal is processed with a pair of lock-in amplifiers and gated integrators to determine the pump-induced absorbance change. FTIR spectra were taken with a Mattson 7020A spectrometer using 25 scans with 1 cm^{-1} resolution.

RM samples were prepared in a manner similar to previous studies.[19] AOT and Brij-30 samples were prepared by adding the appropriate amount of an aqueous NaN_3 solution to a nominally $\omega = 0$ (anhydrous) solution of 0.2 M AOT in *n*-heptane or 0.3 M Brij-30 in cyclohexane. The solution was then sonicated until a clear solution resulted. CTAB is not soluble in anhydrous CH_2Cl_2, so the appropriate amounts of CTAB, CH_2Cl_2, and aqueous azide were mixed until a clear solution resulted. In general, a constant aqueous concentration of azide was used for all values of ω, resulting in a larger sample absorbance for larger ω. Sample path lengths were 250 or 500 μm for RM solutions and 20 or 50 μm for bulk solutions using a static variable path length cell (Harrick) with CaF_2 windows and Teflon spacers. H_2O was obtained from a Milli-Q (Millipore) purification system. All other compounds were purchased from Aldrich and used as received.

Results

FTIR. In a previous publication,[19] we reported results on the FTIR spectra of azide in both H_2O/AOT/*n*-heptane and H_2O/

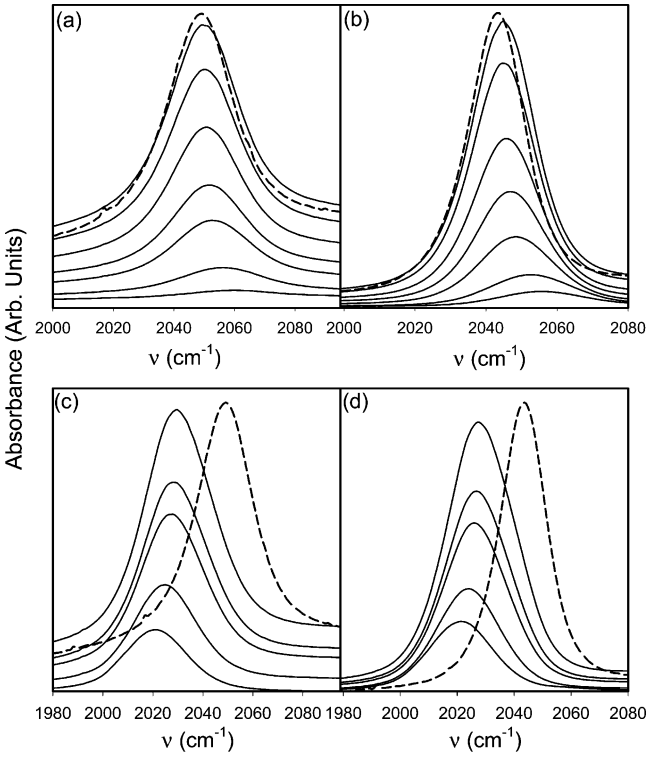

Figure 1. FTIR spectra of antisymmetric stretching band of azide in $\omega = 2$, 3, 5, 7, 10, 13, and 15 (from bottom to top) reverse micelles with 0.2 M AOT/*n*-heptane and 0.25 M azide in H_2O (a) and D_2O (b) and in $\omega = 2$, 3, 5, 6, and 8 reverse micelles with 0.3 M CTAB/CH_2Cl_2 with 0.4 M azide in H_2O (c) and D_2O (d). RM spectra (solid lines) were obtained by subtracting the $\omega = 0$ spectrum for AOT and $\omega = 2$ for CTAB. Azide spectra in bulk H_2O and D_2O spectra (dashed lines) are not subtracted. Spectra are offset because of increasing H_2O or D_2O absorption with increasing ω. Path lengths are 500 μm for the RM samples and 50 and 20 μm for bulk D_2O and H_2O, respectivley.

$CTAB/CH_2Cl_2$ RMs. We found a slight dependence of the azide band peak position on concentration of both surfactant and azide during sample preparations for the present studies. Therefore, we report FTIR spectra obtained under the same conditions as those used for the dynamics measurements. As noted earlier,[19] azide is only stable in AOT RMs at relatively low (<0.25 M) concentrations. Figure 1 shows FTIR spectra of the antisymmetric stretch region of azide in AOT and CTAB RMs containing both H_2O and D_2O. The difference spectra in Figure 1 were obtained by subtracting the corresponding $\omega = 0$ or $\omega = 2$ spectra without azide for AOT and CTAB, respectively. (CTAB is not soluble in anhydrous organic solvents.)

Figure 2 summarizes the ω dependence of the FTIR spectra of the azide antisymmetric stretch for the H_2O and D_2O RM systems studied. AOT RMs were produced from 0.2 M AOT/*n*-heptane by adding 0.25 M NaN_3 for both H_2O and D_2O. For H_2O/AOT, a blue shift of 11 cm^{-1} relative to the bulk H_2O value is seen for $\omega = 2$. As ω increases, the peak position red shifts toward the bulk value coming to within 0.5 cm^{-1} of the bulk value at $\omega = 15$. For D_2O/AOT, a blue shift of 12 cm^{-1} is seen for $\omega = 2$, while at $\omega = 15$, the blue shift is reduced to 1 cm^{-1}. CTAB RMs were made from 0.3 M $CTAB/CH_2Cl_2$ using 0.4 M NaN_3 in both H_2O and D_2O and were stable only up to $\omega = 8$. For H_2O/CTAB RMs, the peak is red shifted 28 cm^{-1} from the bulk value at $\omega = 2$. In the largest CTAB RM studied, $\omega = 8$, the red shift is only reduced to 19 cm^{-1}. In the D_2O/CTAB, a 22 cm^{-1} red shift is observed for $\omega = 2$ while at $\omega = 8$ the band is red shifted by 16.5 cm^{-1}. Brij-30 RMs were made with 0.3 M Brij-30/cyclohexane and 0.4 M NaN_3 in H_2O

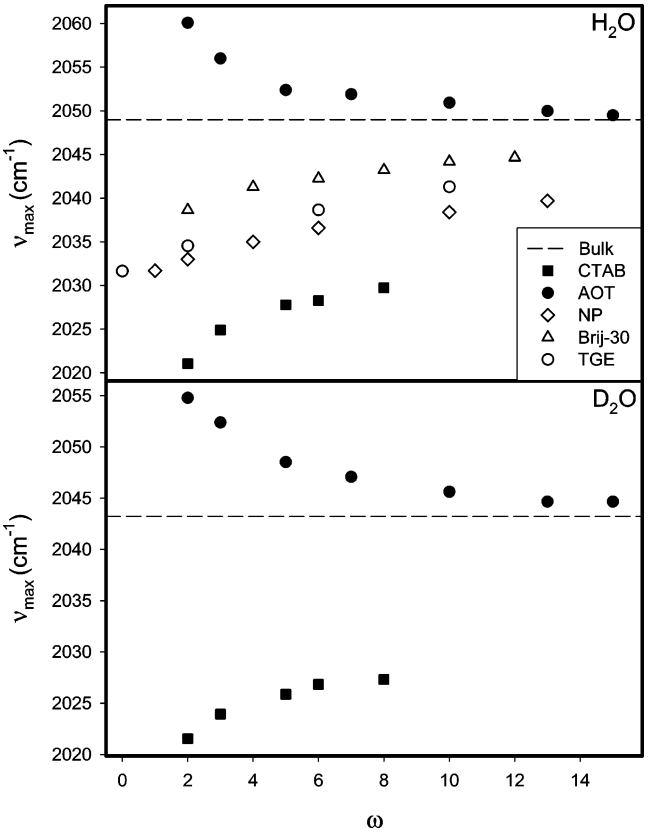

Figure 2. Peak of antisymmetric stretching band of azide as a function of ω for H_2O (top) and D_2O (bottom) containing reverse micelle and TGE mixture solutions. Circles are 0.2 M AOT/*n*-heptane, squares are 0.3 M $CTAB/CH_2Cl_2$, open triangles are 0.3 M Brij-30/cyclohexane, open diamonds are 0.3 M NP/cyclohexane, and open circles are H_2O/TGE mixtures. NP data from ref 19.

only. From $\omega = 2$ to $\omega = 12$, the red shift of the IR band from the bulk value decreases smoothly from 10 to 4.5 cm^{-1}.

For the H_2O/TGE mixtures, ω represents the H_2O:TGE molar ratio. In bulk TGE ($\omega = 0$), the azide IR band is shifted 17 cm^{-1} to the red of the bulk H_2O value. This red shift is 14.5 cm^{-1} for $\omega = 2$ and smoothly decreases to 8 cm^{-1} at $\omega = 10$. As shown in Figure 2, the IR band peak locations in the H_2O/TGE mixtures are between the values seen for the NP and Brij-30 RMs for a given ω.

Vibrational and Rotational Dynamics. T_1 times were determined from decay curves obtained with the relative polarizations of the probe and pump beams oriented at the magic angle (54.7°), which eliminates any polarization dependence. The measured signals were fit to a single-exponential decay convoluted with a Gaussian pulse (~350 fs). Sometimes, an additional instrument-limited component due to coherence or multiphoton processes was observed and was fit by an additional Gaussian term. T_1 times were measured from both bleach and absorption measurements, which agreed within the experimental uncertainties. The peak of the transient absorptions were generally ~20 cm^{-1} to the red of the static absorption. In addition to the T_1 times, the anisotropy decays times, T_r, were also measured for some samples. The anisotropy, $r(t)$, is defined as

$$r(t) = \frac{I_{||}(t) - I_{\perp}(t)}{I_{||}(t) + 2I_{\perp}(t)}$$

where $I_{||}(t)$ and $I_{\perp}(t)$ are the transient signals measured with the relative pump and probe beam polarizations parallel and perpendicular, respectively. The initial value of the anisotropy

TABLE 1: Measured T_1 and T_r Times (in ps) of N_3^- in Ionic RM Systems Studied

	H_2O/AOT/*n*-heptane		D_2O/AOT/*n*-heptane		H_2O/CTAB/$CH_2C\,l_2$		D_2O/CTAB/CH_2Cl_2	
ω	T_1 (ps)	T_r (ps)	T_1 (ps)	T_r (ps)	T_1 (ps)	T_r (ps)	T_1 (ps)	T_r (ps)
2					2.4 ± 0.5	10 ± 5	5.5 ± 0.5	14 ± 4
3	1.0 ± 0.1		3.3 ± 0.4		2.2 ± 0.2		4.8 ± 0.6	
5	0.8 ± 0.1		3.4 ± 0.3	15 ± 5	1.5 ± 0.2	6 ± 2	4.6 ± 0.4	12 ± 2
6					1.5 ± 0.1		4.5 ± 0.5	
8					1.5 ± 0.1	5 ± 1	4.7 ± 0.5	9 ± 2
10	0.7 ± 0.1		3.1 ± 0.3	4.2 ± 0.8				
15	0.8 ± 0.1		3.3 ± 0.4	4.2 ± 0.5				
bulk	0.8 ± 0.1[a]	1.3 ± 0.5[a]	3.2 ± 0.2[b]	4.2 ± 0.8[b]				

[a] Data from ref 55. [b] From this work.

TABLE 2: Measured T_1 Times (in ps) of N_3^- in Nonionic Reverse Micelles and Model TGE/Water Bulk Solutions

	NP[a]	Brij-30	TGE/H_2O
ω	T_1 (ps)	T_1 (ps)	T_1 (ps)
0			3.8 ± 0.2
1	2.5 ± 0.1	1.6 ± 0.2	
2	2.0 ± 0.2	1.3 ± 0.2	1.7 ± 0.1
4	1.7 ± 0.1		
6	1.4 ± 0.2	1.0 ± 0.1	1.2 ± 0.1
10	1.2 ± 0.1	0.9 ± 0.1	1.1 ± 0.1
13	1.0 ± 0.1		
bulk H_2O[b]	0.8 ± 0.1		

[a] Data from ref 56. [b] Data from ref 55.

was near the classically expected value of 0.4 for all cases and the anisotropy decays were fit to a single-exponential decay with time constant T_r. A summary of T_1 and T_r times for the ionic RM systems is given in Table 1. A summary of T_1 times for the nonionic RM systems as well as the H_2O/TGE mixtures is given in Table 2. Representative transients of population and anisotropy decay of azide in bulk D_2O as well as D_2O containing CTAB and AOT RMs are shown in Figure 3. Figure 4 and Figure 5 show the T_1 and T_r times as a function of ω for the H_2O and D_2O reverse RM systems, respectively. Included in Figure 3 are the previous data from the nonionic surfactant NP.[55,56] Measurements in bulk D_2O were repeated on our current apparatus and resulted in a VER relaxation rate that differed slightly and a reorientation time that is significantly shorter than previously reported.[60,62,63]

The measured T_1 times for azide in RMs formed from H_2O and D_2O in AOT are within the uncertainty of the bulk solution values (0.8 ± 0.1 ps for H_2O, 3.2 ± 0.2 ps for D_2O) for all ω. The T_r times for the N_3^-/D_2O/AOT/*n*-heptane system are within the uncertainty of the bulk value of 4.2 ± 0.8 ps for $\omega = 10$ and $\omega = 15$, but a longer T_r time of 15 ± 5 ps is found for $\omega = 5$. For azide in CTAB, the measured T_1 and T_r times are longer than the bulk in all cases. For H_2O, T_1 is 2.5 ps at $\omega = 2$ and decreases to about 1.5 ps at $\omega = 5$ and remains constant for further increases in ω. Similar behavior is seen for D_2O, with T_1 times of 5.5 ps at $\omega = 2$ and 4.5 ps for $\omega \geq 5$. For both solvent isotopomers, the T_r times show a general decrease with increasing ω; however, the large uncertainties prevent extraction of any more detailed trends. For Brij-30, the T_1 time is about twice the bulk value for $\omega = 2$ and smoothly approaches the bulk value as ω increases and is indistinguishable from the bulk value at $\omega = 10$. Figure 6 shows T_1 as a function of ω for the nonionic RMs as well as for the H_2O/TGE mixtures. For the H_2O/TGE mixtures, there is a big jump between bulk TGE at 3.8 ps and $\omega = 2$ at 1.7 ps. However, the T_1 times then smoothly approach the bulk H_2O values as ω increases, reaching 1.1 ps at $\omega = 10$. As shown in Figure 6, the T_1 times of the H_2O/TGE mixtures are within the range spanned by the T_1 times seen in the nonionic NP and Brij-30 RMs. Figure 7 shows a plot of

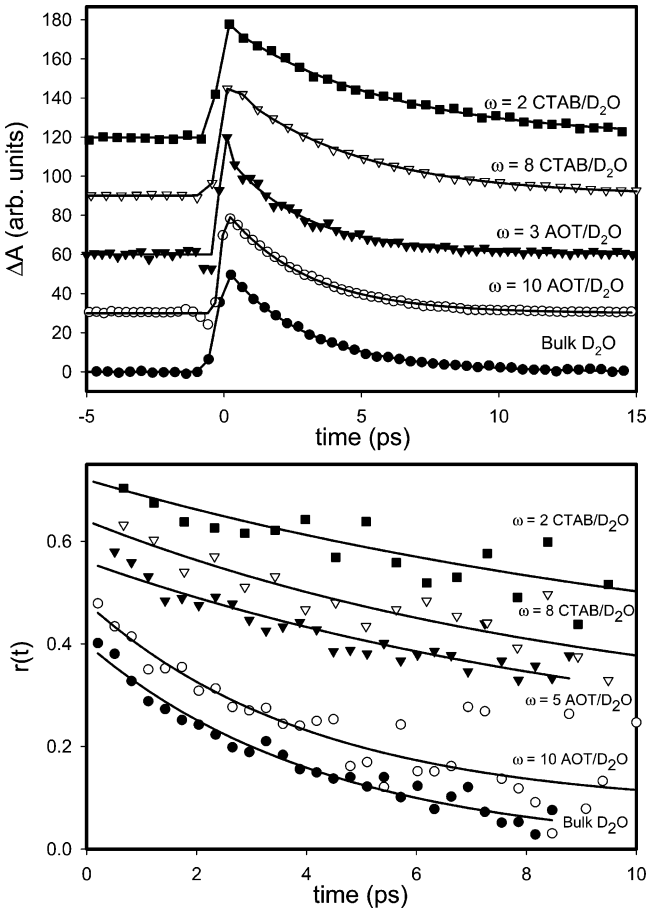

Figure 3. Representative transients (points) of population (top) and anisotropy (bottom) decay of azide in bulk D_2O and D_2O containing AOT and CTAB reverse micelles. Also included are fits to exponential decays (lines). The curves are offset for clarity. From top to bottom, the transients are transient bleach (TB) at 2020 cm^{-1}, transient absorption (TA) at 1985 cm^{-1}, TA at 2020 cm^{-1}, TB at 2038 cm^{-1}, TB at 2045 cm^{-1}, TA at 1990 cm^{-1}, TB at 2030 cm^{-1}, TB at 2047 cm^{-1}, TB at 2045 cm^{-1}, and TB at 2045 cm^{-1}.

VER rate, $k_1 = 1/T_1$, versus vibrational frequency for all H_2O and D_2O RM systems studied as well as for bulk solution.

Discussion

Background and Previous RM Studies. Previous studies of azide in RMs using the nonionic surfactant NP suggested that the ion resided in the center of the water pool.[55,56] The reduced mobility and polarity of the water within the RM was reflected in rotational and vibrational relaxation dynamics that were slower than seen in bulk solution. The reduction in VER rate was less than has been observed for solvation dynamics, only a factor of 3 for $\omega = 1$, compared to at least an order of

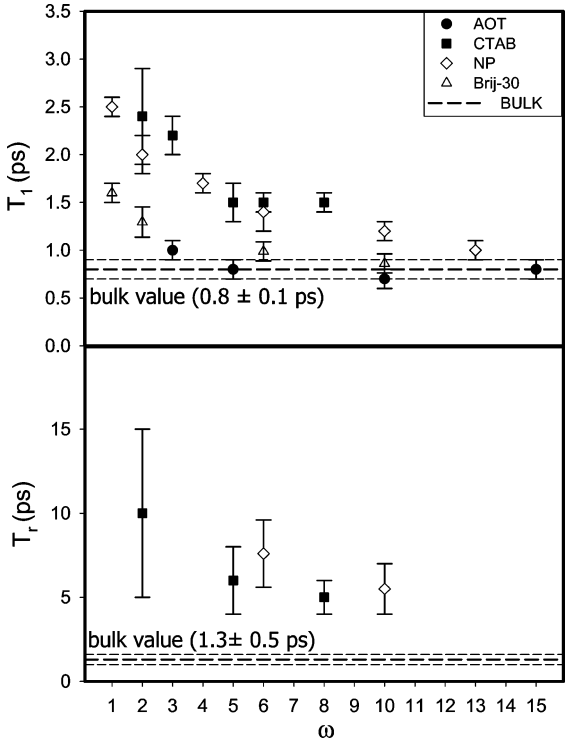

Figure 4. T_1 and T_r times for azide in H_2O containing reverse micelle systems as a function of ω. Circles are 0.2 M AOT/*n*-heptane, squares are 0.3 M CTAB/CH_2Cl_2, open triangles are 0.3 M Brij-30/cyclohexane, and open diamonds are 0.3 M NP/cyclohexane. NP data from refs 55 and 56.

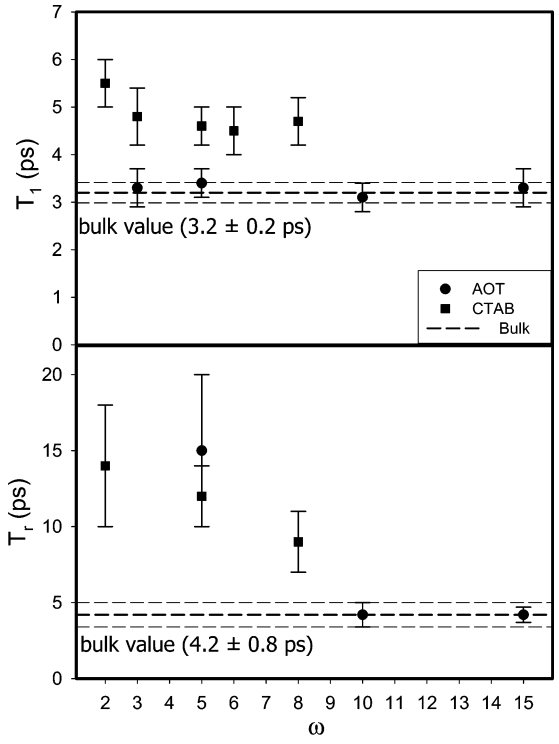

Figure 5. T_1 and T_r times for azide in D_2O containing reverse micelle systems as a function of ω. Circles are 0.2 M AOT/*n*-heptane and squares are 0.3 M CTAB/CH_2Cl_2.

magnitude or greater decrease in the rate of solvation dynamics.[34−45] This is not unexpected because of the more local nature of VER as compared to the longer range solvent motions involved in solvation dynamics. Consistent with this picture was a greater reduction in the reorientation rate, with T_r increasing

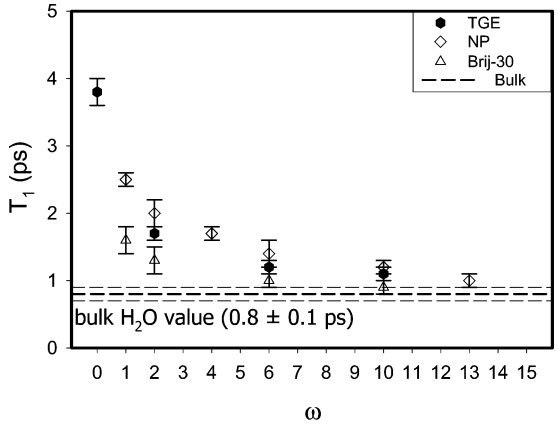

Figure 6. T_1 times for azide in H_2O containing nonionic reverse micelle systems and H_2O/TGE mixtures as a function of ω. Open triangles are 0.3 M Brij-30/cyclohexane, open diamonds are 0.3 M NP/cyclohexane, and hexagons are H_2O/TGE mixtures. NP data from ref 56.

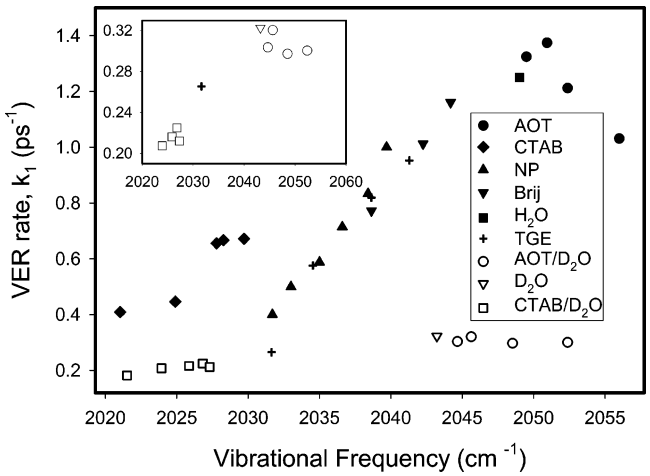

Figure 7. VER rate, $k_1 = 1/T_1$, vs vibrational frequency for azide in reverse micelles and bulk solutions. Circles are 0.2 M AOT/*n*-heptane, squares are 0.3 M CTAB/CH_2Cl_2, triangles pointing up are 0.3 M Brij-30/cyclohexane, diamonds are 0.3 M NP/cyclohexane, hexagons are H_2O/TGE mixtures, and triangles pointing down are bulk water. Closed symbols are for H_2O while open symbols are for D_2O. Shown in the inset is a larger view of the D_2O data. NP and bulk H_2O data from ref 56.

by a factor of an order of magnitude for small RMs. The values measured for T_1 and T_r approach those observed in the bulk as ω increasees, consistent with a more bulklike water pool as the RM size increases. In addition, the correlation between azide VER rate and the vibrational frequency seen in a range of bulk solvents also applied to NP RMs. However, the inverse correlation between T_r and T_1 seen for bulk solvents, both of which are related to the strength of solute−solvent coupling, is not preserved in RMs.[55,60,61] This result is consistent with the established idea that the environment inside a RM water pool is highly restricted, inhibiting rotation and overwhelming effects such as those in the bulk that are due to solvent−solute coupling. The location of azide in the NP water pool is still somewhat ambiguous, hindering interpretation of the results. Extension of these studies to RMs using the ionic surfactants CTAB and AOT, where Coulombic effects may be expected to play a major role in determining the location of azide within the RM, as well as Brij-30, with a shorter poly-oxo chain than NP, results in different dynamics that provides further evidence of the location of the azide ion in the different RM water pools.

AOT. On the basis of Coulombic factors alone and neglecting possible counterion effects, RMs constructed from the anionic

surfactant AOT should favor placement of the anionic probe azide in the center of the water pool. This behavior is consistent with simulations of I_2^- in AOT.[30] The low solubility of azide in AOT RMs could be due to the Coulombic repulsion limiting the number of azide ions that may reside in a single RM. The core of the water pool is thought to be the region of the water pool with the most bulklike properties.[29,30,34−45] Therefore, among the various RM systems, azide in AOT should exhibit dynamics most similar to the bulk. In fact, behavior very similar to the bulk is observed. At all values of ω, T_1 times were within the uncertainty of the bulk for both H_2O and D_2O containing RMs. VER is faster in AOT than the previously studied[55,56] NP RMs, especially for small ω. T_r times were within the uncertainty of the bulk for D_2O containing RMs for $\omega = 10$ and 15. However, a longer T_r time was measured for the smallest RM studied, $\omega = 5$. T_r times in H_2O containing RMs were not reliable because of the short T_1 time.

These results indicate that the azide ion is most likely located in the most bulklike region of the AOT RMs, the center of the water pool. The similarity of the dynamics in the RMs to bulk dynamics indicates that the ion−solvent interactions in the core region of the water pool are very similar to bulk water. The small size of azide increases the probability that it is situated in the core region of the water pool, so that the ion should not be directly affected by the outer water layers nor should it perturb the RM structure. Simulations[29] and experiments[12,64] have suggested that the bound layer is within 4−5 Å of the surfactant headgroups. Bulklike free water fills in the remaining portion of the RM interior. The radius of the AOT RMs studied range from ∼10 Å ($\omega = 2$) to >20 Å ($\omega = 15$),[29] leaving a significant bulk water pool, especially for the larger RMs. For $\omega = 5$, with a radius of ∼15 Å, interactions between the outer layers and the solvation shell are apparently strong enough to restrict the lateral movement of azide, resulting in a long T_r time. The location of azide is consistent with the Coulombic repulsion between the solute and the surfactant. Similar repulsive interactions have been reported for other RM systems where the solute and surfactant have the same charge.[57,58]

The static spectra we measured are also consistent with a core location of the azide ion. A relatively small blue shift is observed in AOT RMs. The shift is not only smaller but is of the opposite sign than is seen for the other RM systems. It is also more concentration dependent than the other RM systems because azide is not well solubilized in AOT RMs. Results from bulk solvent studies indicate that reducing the polarity of the solvation environment should induce a red shift, not a blue shift as is observed, in the azide ν_3 vibrational band.[60,61] The blue shift may be attributed to the high ionic strength of the water pool because of the Na^+ counterions from AOT.[19] The high ionic strength suggests that the long T_r time for the $\omega = 5$ RM may be due to ion pairing. Ion pairing of azide in DMSO resulted in similar T_1 times but longer T_r times compared to the free ion in the same solvent.[65] To determine if ion pairing might account for the spectral shifts and dynamics we observe, experiments were performed in a nearly saturated (0.6−0.7 M) solution of NaCl with 0.2 M NaN_3 in D_2O. A static spectral blue shift of ∼4 cm^{-1} was observed as in the RMs as previously reported for H_2O solutions;[19] however, the T_1 and T_r times were nearly indistinguishable from bulk D_2O. In addition, contact ion pairs in DMSO had much larger spectral blue shifts.[65,66] Evidently, our observations cannot be attributed to the presence of azide ion pairs in the RMs.

An additional possibility that we cannot rule out in the present experiments is that the presence of azide is affecting the RM structure. So far, we have assumed that azide has no impact on the RM structure on the basis of the small size of the ion. In previous work on NP RMs,[19] we found no evidence of size effects due to the presence of azide. However, the Coulombic repulsion between the azide ion and the AOT surfactant headgroups may alter the RM size distribution resulting in larger RM water pools than in the absence of azide. Similar RM size distortion was observed for $Ru(pby)_3^{2+}$ with a cationic surfactant.[57] The small solute concentration dependence of the FTIR band peak positions may suggest an altering of the RM size distribution, but the shifts are similar to what is observed in bulk solution as the ionic strength is changed. Even if the size distribution is altered, the primary conclusion, that anionic azide prefers a bulklike environment in AOT RMs, does not change.

CTAB. For the azide in cationic CTAB RMs, Coulombic attraction draws the anion toward the surfactant ammonium headgroup. If azide is located at or near the surfactant wall, it resides in an environment that is significantly different than the bulk. This may result in spectral and dynamical properties that exhibit a weak dependence on ω since the environment should be insensitive to water content and RM size. In fact, this is observed for the static spectral shifts of the antisymmetric stretching band. There is a large red shift of azide in CTAB RMs compared to the bulk frequency and it does not depend strongly on ω. Unlike in the other RMs, the vibrational frequency does not approach the bulk value for high ω and is about 20 cm^{-1} lower than in bulk water for even the largest ω studied. The vibrational dynamics observed show a similar trend. The VER times are appreciably different than in bulk aqueous solutions and are relatively insensitive to ω, reinforcing the idea that the anion is at or near the interfacial region of the RM. For the smallest H_2O RM studied, $\omega = 2$, the T_1 time is longer than the bulk by a factor of about 3 and is similar to the value seen for NP. In larger ω RMs, the T_1 times are somewhat shorter than previously measured in NP RMs,[55,56] but unlike NP, the T_1 times appear to level off after $\omega = 5$. Similar behavior is seen for both H_2O and D_2O containing RMs, although the relative increase in T_1 time as compared to the bulk is less for the D_2O system. Even for the largest RMs, the T_1 times are significantly longer than those seen in the bulk, nearly double in the H_2O case and 50% longer in the D_2O case. The T_r times are similar to what has been observed for NP, although the large uncertainties make identification of trends difficult.

These results provide evidence about the location of azide in CTAB RMs. The static spectral shifts are largest for CTAB. The T_1 and T_r dynamics are slower than in the bulk and T_1 appears to level off with increasing ω. These results imply a strong interaction with the surfactant wall. The reorientation time is much faster than expected for the RM as a whole, which is about 1 ns.[37,41,67] This could be because the ion is restricted to the less mobile outer layer of water, which most likely has a significant local concentration of bromide counterions that further restrict motion, rather than directly attached to the surfactant headgroups themselves. For the range of ω studied, the water pool radii range from ∼10 Å to ∼20 Å with a 10 Å outer layer of bound water.[11,12,14] This provides a region with significantly hindered mobility that is large enough for azide to reside in without being directly bound to surfactant headgroups. However, attachment to the headgroups is still possible if it inhibits but does not prevent reorientation. Since T_r is much longer than T_1, the anisotropy decay is difficult to determine because the signal decays via VER before there is appreciable anisotropy loss. Our data cannot differentiate between one relatively slow component due to reorientation in the restricted

outer layer of water and a two-component decay due to partial reorientation within the RM and reorientation of the entire RM.[37,41,59,68] Our results are consistent with the anion being near the interface because of Coulombic attraction between the anionic azide probe and the cationic surfactant. Similar behavior has been seen for oppositely charged solute−surfactant systems.[34,49,50,57,58] These results resemble what has been observed for hydrophobic probes, which tend to be located in the interface rather than the water pool.[27,44] However, because of the small size and charged nature of azide and considering the results from other RM systems, hydrophobic interactions are probably not a factor. The ω dependence of T_1 for azide in low ω CTAB RMs does reveal a change in the ion's environment. Even if azide were attached to the wall, it would still be indirectly affected by changes in the outer layer of the water because of exposure to the water pool on one side of the ion. The initial T_1 dependence could be due to changes in the properties of the outer water layer until the multilayer structure is fully developed. An alternative explanation is that the change in curvature of the RM wall changes enough at small ω to influence the VER rates. A combination of both factors could also play a role. It is difficult to distinguish between these possibilities on the basis of our data.

Brij-30 and NP. The results in the ionic RMs, as well as the nonionic Brij-30 RMs, help to clarify the location of azide in the previously studied NP RM system. NP and Brij-30 differ significantly from both AOT and CTAB in that the interfacial region of nonionic RMs is not as well defined. NP and Brij-30 have poly-oxo chains terminating with an OH that form the hydrophilic end rather than a single charged headgroup as in CTAB and AOT. In the nonionic case, water and azide can penetrate into the region of the poly-oxo chains, especially for small ω in which water pools may not be fully formed because of water solvating the long poly-oxo chains instead of azide. For surfactants with similar hydrophilic poly-oxo chains, water pools are not yet formed for small ω RMs.[26,27,31,69−71] Previous measurements of NP RM size in our lab using fluorescence quenching revealed an increase in the RM radius from 13 Å at $\omega = 3$ to 35 Å at $\omega = 10$. These radii most likely correspond to the size of the entire micelle interior, including the poly-oxo chains, rather than the size of the water pool. Interactions with the chains would result in a less polar environment, an associated increase in the T_1 time, and a significant increase in T_r. This suggests a reason for the similarity between NP and CTAB for small ω, where significant interaction with the surfactant could account for the similar T_1 and T_r times. However, as ω increases, a water pool does begin to form for NP RMs after fully solvating the poly-oxo chains, although the polar core pool may still have a poorly defined interface. The hydrophilic portions of Brij-30 and NP are similar, differing only in length, that is, number of poly-oxo units. The poly-oxo chain is shorter in Brij-30, approximately 4 repeat units, than in NP, approximately 7 repeat units. If water pool formation occurs after the poly-oxo units are hydrated, this should occur for a smaller value of ω for Brij-30 than NP. The azide ion is expected to favor the water pool when it is formed, leading to dynamics that approach bulk behavior for large ω, including both T_1 and T_r times. Since water pool formation is expected to occur at a smaller ω for Brij-30 than for NP, faster VER dynamics are expected for Brij-30 than for NP for a given value of ω. This is what we observe; the dynamics are slower in NP RMs than in Brij-30 RMs. Similar behavior was observed in solvation dynamics studies of Brij-30 and Triton-X, which has 10 oxo groups to solvate.[37] In addition, the static spectral red shift from the bulk is also larger for NP RMs, consistent with a stronger interaction with the poly-oxo chains for the longer-chained surfactant. The VER times in nonionic Brij-30 RMs fall between those of cationic CTAB and anionic AOT, consistent with the present picture of the RM−solute interaction. For small ω, the T_1 time in CTAB is similar to that of NP but not Brij-30. This is consistent with a stronger wall interaction in NP because of the longer poly-oxo chains requiring more water molecules to solvate, leaving fewer water molecules to solvate the azide anion.

This picture is also consistent with the behavior reported for NCS^- in NP.[55] NCS^- is much less hydrophilic than azide, as reflected by its higher solubility in organic solvents. Overall, the IR active stretch of NCS^-, which is primarily C−N stretch in nature, has smaller solvent shifts than azide. However, NCS^- undergoes a significant shift in NP RMs and shows little variation with ω. In addition, T_r is much longer for NCS^- in NP than azide in NP RMs of similar size. These factors suggest NCS^- has a stronger preference for the interfacial region and that azide prefers the water pool once it is formed.

Tri(ethylene glycol) Monomethyl Ether. For further confirmation of the above picture, experiments were performed in mixtures of water and a model of the hydrophilic portion of the nonionic surfactants. The model species, tri(ethylene glycol) monomethyl ether (TGE), has three repeat units in the polyoxo chain as compared to four and seven for Brij-30 and NP, respectively. Experiments were performed at molar ratios intended to simulate concentrations in the interior of the RM. For the H_2O/TGE mixtures, ω is defined as the molar ratio of H_2O to TGE. As seen in Figure 6, similar behavior is seen as a function of ω for all three nonionic systems, Brij-30 RMs, NP RMs, and H_2O/TGE mixtures. The T_1 times for the H_2O/TGE mixtures are between the T_1 times for NP and Brij-30 RMs. On the basis of the chain lengths alone, longer T_1 times would be expected for NP RMs, as is observed. However, for Brij-30, T_1 times that are similar to or slightly longer than seen for H_2O/TGE mixtures would be expected because of the difference in poly-oxo chain lengths. However, in all cases the T_1 times for the H_2O/TGE mixtures are significantly longer than for Brij-30 RMs and are close to the values seen for NP RMs even though the poly-oxo chains of TGE are much shorter. This suggests a stronger segregation between water and the poly-oxo chains and a greater ability to form water pools in the interior of the nonionic RMs than in the H_2O/TGE mixtures, where a uniform mixture is expected. This type of behavior has been suggested in nonionic RMs through the existence of a nonuniform distribution of water polarity, where interior water molecules have a higher polarity than water molecules that are within the poly-oxo chains.[16,59,69]

We have also recently performed VER experiments of several cyanoferrates in RMs and H_2O/TGE mixtures.[72] The overall trends with surfactant charge are very similar to what is observed with azide, but they differ in some of the details. These differences can mainly be attributed to the larger size and different hydrophilic nature of the cyanoferrate molecules studied. In addition, the vibrational dynamics of the cyanoferrates in bulk solution are more complex than for azide,[73] which complicates attempts to generalize regarding the effect of surfactant charge on solute chemical behavior in RMs. Ferrocyanide is not soluble in methanol or bulk TGE and is soluble in H_2O/TGE mixtures only for ω greater than 15. The solubility of ferrocyanide in Brij-30 RMs, but not in NP RMs, provides evidence for a greater ability to form water pools in the shorter-chained Brij-30 RMs. However, it is unclear if there are any

changes to the RM structure because of the solutes that would prevent a direct comparison of the two systems.

Rate-Shift Correlations. Previous studies of the azide ion in several solvents have revealed a correlation between the vibrational frequency shift from the gas phase[74] and the VER rate.[60,61] Both quantities are related to the strength of the solute−solvent interaction. The correlation between solvent-shifted vibrational frequency and VER rate is well-established in bulk solvents, suggesting that the solute−solvent interactions that mediate these observables depend similarly on the solvent properties. The correlation was also found to hold for studies in NP RMs containing H_2O.[55,56] In contrast, in ion pairs with metal cations in DMSO, the azide frequency is blue shifted without any associated change in the VER rate, resulting in a breakdown of the correlation between rate and frequency.[65] This suggests an additional interaction in the ion pairs that is absent in bulk solvent that affects the frequency differently than the VER rate. Therefore, we consider the correlation between the azide vibrational frequency and VER rate as an empirical measure of ion solvation, which can be used to compare between different RMs and to bulk solution. In light of these results, we evaluated the degree of correlation between frequency and VER rate measured for azide in the present study to identify unique aspects of the solvation environment. We have plotted the VER rate ($k_1 = 1/T_1$) against the vibrational frequency for bulk H_2O and D_2O as well as for all of the RM and TGE systems studied, as shown in Figure 7. The results yield an overall positive correlation for the samples. The correlation is better within the H_2O or D_2O containing systems than when both are considered together. Not all the systems fall on a single line and the points for different RMs are segregated, reinforcing the suggestion made previously that RMs with different charge result in different ion solvation environments. For the systems containing H_2O, the points for CTAB RMs are above the line established by the other samples because the VER times are longer for their vibrational frequency compared to the others. The results for the AOT RMs are clustered near the bulk water value. The points with low ω have a higher frequency or apparently slower rate; these are the AOT samples with blue-shifted frequency without an associated increase in VER rate. However, the nonionic systems show a good linear correlation; the nonionic RM and TGE samples exhibit similar behavior in terms of the rate-shift behavior regardless of ω. The CTAB results suggest that azide is in a different environment than in the nonionic and bulk systems. The difference is most likely due to interaction with the cationic micelle and, similar to the ion pair results, the static and dynamical quantities are affected differently by this additional, mostly ionic, interaction. The correlation breaks down when comparing the H_2O and D_2O systems. Recently, we have extended the range of bulk solvents in which the VER dynamics of azide has been studied and the results provide further evidence for a linear correlation between vibrational frequency and VER rate with the exception of H_2O, which is anomalously fast.[75] The results in D_2O, however, do follow the linear correlation with other bulk solvents. This is consistent with the present results in which those containing H_2O are much faster than those with D_2O when comparing systems with similar vibrational frequencies. This could also explain why the rate in bulk TGE appears too slow compared to the H_2O systems and fits more in line with the D_2O data.

Conclusions

We have performed VER measurements on a small azide ion, N_3^-, in anionic and cationic RMs. These results have been compared to dynamics in both bulk and nonionic RMs. The VER dynamics depend on the surfactant charge. For anionic AOT, the dynamics are indistinguishable from bulk aqueous solution. For cationic CTAB, a reduction in VER rate by a factor of 3 is observed for the smallest RM, similar to nonionic NP RMs. However, unlike NP, in which the VER rate smoothly approaches the bulk as ω is increased, the VER rate for CTAB RMs reaches a plateau around $\omega = 5$. For nonionic Brij-30 RMs, a reduction in VER rate by a factor of 2 is seen for the smallest RMs, and the VER rate smoothly approaches the bulk as the RM size is increased, becoming indistinguishable from the bulk at $\omega = 10$. The trends in T_1 times are similar to trends seen in the static IR absorptions. Although the T_r times are lengthened more than the VER times, there appear to be similar trends with respect to ω. The trends in T_r are much harder to identify because of their larger uncertainties. Overall, the T_r times in CTAB, as in NP, are significantly slower than those seen in bulk solution. For D_2O containing AOT RMs, T_r times are indistinguishable from the bulk except for the smallest RM studied, $\omega = 5$.

The variation in VER dynamics we have observed for differently charged RMs is attributed to the ion location in the RMs. For neutral surfactants with long poly-oxo chains, such as NP and Brij-30, azide appears to interact with the chains for small ω, especially for the longer-chained NP surfactant. As ω increases and the water pool becomes better defined, azide begins to prefer a location within the water pool, allowing bulklike behavior to be approached for large RMs. For anionic AOT, azide appears to prefer the center of the water pool for all values of ω, resulting in bulklike dynamics in all cases. For CTAB, a strong interaction between the cationic surfactant and anionic azide prevents azide from residing in the interior of the water pool. Instead, azide resides in the less polar outer layers of water where solvent motion is greatly hindered, or azide is attached to the surfactant headgroup. In either case, bulklike behavior is not achieved even for large RMs.

Acknowledgment. Support for this work was provided by the Office of Naval Research through the Naval Research Laboratory. G.M.S. acknowledges the Naval Research Laboratory − American Society for Engineering Education Postdoctoral Fellowship program. K.D. acknowledges the Naval Research Laboratory − National Research Council Research Associateship program. We would like to thank Edward Castner and Nancy Levinger for helpful discussions.

References and Notes

(1) Bellissent-Funel, M. C. *J. Phys.: Condens. Matter* **2001**, *13*, 9165−9177.
(2) Weik, M. *Eur. Phys. J. E* **2003**, *12*, 153−158.
(3) Nandi, N.; Bhattacharyya, K.; Bagchi, B. *Chem. Rev.* **2000**, *100*, 2013−2045.
(4) Scodinu, A.; Fourkas, J. T. *J. Phys. Chem. B* **2002**, *106*, 10292−10295.
(5) Hazra, P.; Chakrabarty, D.; Chakraborty, A.; Sarkar, N. *Chem. Phys. Lett.* **2004**, *388*, 150−157.
(6) Bellissent-Funel, M. C. *Eur. Phys. J. E* **2003**, *12*, 83−92.
(7) Rovere, M.; Gallo, P. *Eur. Phys. J. E* **2003**, *12*, 77−81.
(8) Bhattacharyya, K.; Bagchi, B. *J. Phys. Chem. A* **2000**, *104*, 10603−10613.
(9) Douhal, A. *Chem. Rev.* **2004**, *104*, 1955−1976.
(10) Bohidar, H. B.; Behboudnia, M. *Colloids Surf., A* **2001**, *178*, 313−323.
(11) Das, P. K.; Chaudhuri, A.; Saha, S.; Samanta, A. *Langmuir* **1999**, *15*, 4765−4772.
(12) Giustini, M.; Palazzo, G.; Colafemmina, G.; DellaMonica, M.; Giomini, M.; Ceglie, A. *J. Phys. Chem.* **1996**, *100*, 3190−3198.

(13) Petit, C.; Bommarius, A. S.; Pileni, M. P.; Hatton, T. A. *J. Phys. Chem.* **1992**, *96*, 4653−4658.
(14) Lang, J.; Mascolo, G.; Zana, R.; Luisi, P. L. *J. Phys. Chem.* **1990**, *94*, 3069−3074.
(15) Lang, J.; Jada, A.; Malliaris, A. *J. Phys. Chem.* **1988**, *92*, 1946−1953.
(16) Vasilescu, M.; Caragheorgheopol, A.; Caldararu, H. *Adv. Colloid Interface Sci.* **2001**, *89*, 169−194.
(17) Griffiths, P. C.; Paul, A.; Heenan, R. K.; Penfold, J.; Ranganathan, R.; Bales, B. L. *J. Phys. Chem. B* **2004**, *108*, 3810−3816.
(18) Griffiths, P. C.; Cheung, A. Y. F.; Farley, C.; Paul, A.; Heenan, R. K.; King, S. M.; Pettersson, E.; Stilbs, P.; Ranganathan, R. *J. Phys. Chem. B* **2004**, *108*, 1351−1356.
(19) Zhong, Q.; Steinhurst, D. A.; Carpenter, E. E.; Owrutsky, J. C. *Langmuir* **2002**, *18*, 7401−7408.
(20) Onori, G.; Santucci, A. *J. Phys. Chem.* **1993**, *97*, 5430−5434.
(21) Brubach, J. B.; Mermet, A.; Filabozzi, A.; Gerschel, A.; Lairez, D.; Krafft, M. P.; Roy, P. *J. Phys. Chem. B* **2001**, *105*, 430−435.
(22) Jain, T. K.; Varshney, M.; Maitra, A. *J. Phys. Chem.* **1989**, *93*, 7409−7416.
(23) Macdonald, H.; Bedwell, B.; Gulari, E. *Langmuir* **1986**, *2*, 704−708.
(24) Gonzalez-Blanco, C.; Rodriguez, L. J.; Velazquez, M. M. *J. Colloid Interface Sci.* **1999**, *211*, 380−386.
(25) Correa, N. M.; Biasutti, M. A.; Silber, J. J. *J. Colloid Interface Sci.* **1996**, *184*, 570−578.
(26) Kawai, T.; Shindo, N.; Konno, K. *Colloid Polym. Sci.* **1995**, *273*, 195−199.
(27) Qi, L. M.; Ma, J. M. *J. Colloid Interface Sci.* **1998**, *197*, 36−42.
(28) Faeder, J.; Albert, M. V.; Ladanyi, B. M. *Langmuir* **2003**, *19*, 2514−2520.
(29) Faeder, J.; Ladanyi, B. M. *J. Phys. Chem. B* **2000**, *104*, 1033−1046.
(30) Faeder, J.; Ladanyi, B. M. *J. Phys. Chem. B* **2001**, *105*, 11148−11158.
(31) Allen, R.; Bandyopadhyay, S.; Klein, M. L. *Langmuir* **2000**, *16*, 10547−10552.
(32) Senapati, S.; Berkowitz, M. L. *J. Chem. Phys.* **2003**, *118*, 1937−1944.
(33) Brown, D.; Clarke, J. H. R. *J. Phys. Chem.* **1988**, *92*, 2881−2888.
(34) Corbeil, E. M.; Levinger, N. E. *Langmuir* **2003**, *19*, 7264−7270.
(35) Levinger, N. E. *Curr. Opin. Colloid Interface Sci.* **2000**, *5*, 118−124.
(36) Levinger, N. E. *Science* **2002**, *298*, 1722−1723.
(37) Pant, D.; Levinger, N. E. *Langmuir* **2000**, *16*, 10123−10130.
(38) Pant, D.; Riter, R. E.; Levinger, N. E. *J. Chem. Phys.* **1998**, *109*, 9995−10003.
(39) Riter, R. E.; Undiks, E. P.; Kimmel, J. R.; Levinger, N. E. *J. Phys. Chem. B* **1998**, *102*, 7931−7938.
(40) Riter, R. E.; Undiks, E. P.; Levinger, N. E. *J. Am. Chem. Soc.* **1998**, *120*, 6062−6067.
(41) Riter, R. E.; Willard, D. M.; Levinger, N. E. *J. Phys. Chem. B* **1998**, *102*, 2705−2714.
(42) Willard, D. M.; Levinger, N. E. *J. Phys. Chem. B* **2000**, *104*, 11075−11080.
(43) Willard, D. M.; Riter, R. E.; Levinger, N. E. *J. Am. Chem. Soc.* **1998**, *120*, 4151−4160.
(44) Hazra, P.; Chakrabarty, D.; Chakraborty, A.; Sarkar, N. *Chem. Phys. Lett.* **2003**, *382*, 71−80.
(45) Hazra, P.; Sarkar, N. *Chem. Phys. Lett.* **2001**, *342*, 303−311.
(46) Jiang, Y. B.; Jin, M. G. *Spectrochim. Acta, Part A* **2000**, *56*, 623−627.
(47) Datta, A.; Mandal, D.; Pal, S. K.; Bhattacharyya, K. *J. Phys. Chem. B* **1997**, *101*, 10221−10225.
(48) Mandal, D.; Pal, S. K.; Datta, A.; Bhattacharyya, K. *Anal. Sci.* **1998**, *14*, 199−202.
(49) Vinogradov, A. M.; Tatikolov, A. S.; Costa, S. M. B. *Phys. Chem. Chem. Phys.* **2001**, *3*, 4325−4332.
(50) Datta, A.; Mandal, D.; Pal, S. K.; Bhattacharyya, K. *Chem. Phys. Lett.* **1997**, *278*, 77−82.
(51) Fioretto, D.; Freda, M.; Mannaioli, S.; Onori, G.; Santucci, A. *J. Phys. Chem. B* **1999**, *103*, 2631−2635.
(52) Mittleman, D. M.; Nuss, M. C.; Colvin, V. L. *Chem. Phys. Lett.* **1997**, *275*, 332−338.
(53) Seifert, G.; Patzlaff, T.; Graener, H. *Phys. Rev. Lett.* **2002**, *88*, 147402.
(54) Patzlaff, T.; Janich, M.; Seifert, G.; Graener, H. *Chem. Phys.* **2000**, *261*, 381−389.
(55) Zhong, Q.; Baronavski, A. P.; Owrutsky, J. C. *J. Chem. Phys.* **2003**, *119*, 9171−9177.
(56) Zhong, Q.; Baronavski, A. P.; Owrutsky, J. C. *J. Chem. Phys.* **2003**, *118*, 7074−7080.
(57) Rack, J. J.; McCleskey, T. M.; Birnbaum, E. R. *J. Phys. Chem. B* **2002**, *106*, 632−636.
(58) Saez, M.; Abuin, E. A.; Lissi, E. A. *Langmuir* **1989**, *5*, 942−947.
(59) Dutt, G. B. *J. Phys. Chem. B* **2004**, *108*, 805−810.
(60) Li, M.; Owrutsky, J.; Sarisky, M.; Culver, J. P.; Yodh, A.; Hochstrasser, R. M. *J. Chem. Phys.* **1993**, *98*, 5499−5507.
(61) Owrutsky, J. C.; Raftery, D.; Hochstrasser, R. M. *Annu. Rev. Phys. Chem.* **1994**, *45*, 519−555.
(62) Owrutsky, J. C.; Kim, Y. R.; Li, M.; Sarisky, M. J.; Hochstrasser, R. M. *Chem. Phys. Lett.* **1991**, *184*, 368−374.
(63) Hamm, P.; Lim, M.; Hochstrasser, R. M. In *Ultrafast Phenomena XI*; Elsaesser, T., Fujimoto, J. G., Wiersma, D. A., Zinth, W., Eds.; Springer-Verlag: Berlin, 1998; pp 514−516.
(64) Maitra, A. *J. Phys. Chem.* **1984**, *88*, 5122−5125.
(65) Zhong, Q.; Owrutsky, J. C. *Chem. Phys. Lett.* **2004**, *383*, 176−180.
(66) Le Borgne, C.; Illien, B.; Beignon, M.; Chabanel, M. *Phys. Chem. Chem. Phys.* **1999**, *1*, 4701−4706.
(67) Krishnakumar, S.; Somasundaran, P. *J. Colloid Interface Sci.* **1994**, *162*, 425−430.
(68) Dutt, G. B. *J. Phys. Chem. B* **2004**, *108*, 3651−3657.
(69) Caldararu, H.; Caragheorgheopol, A.; Vasilescu, M.; Dragutan, I.; Lemmetyinen, H. *J. Phys. Chem.* **1994**, *98*, 5320−5331.
(70) Dutt, G. B. *J. Phys. Chem. B* **2004**, *108*, 7944−7949.
(71) Kimura, N.; Umemura, J.; Hayashi, S. *J. Colloid Interface Sci.* **1996**, *182*, 356−364.
(72) Sando, G. M.; Dahl, K.; Owrutsky, J. C. *J. Phys. Chem. A* **2004**, submitted.
(73) Sando, G. M.; Zhong, Q.; Owrutsky, J. C. *J. Chem. Phys.* **2004**, *121*, 2158−2168.
(74) Owrutsky, J.; Rosenbaum, N.; Tack, L.; Gruebele, M.; Polak, M.; Saykally, R. J. *Philos. Trans. R. Soc. London, Ser. A* **1988**, *324*, 97−108.
(75) Dahl, K.; Sando, G. M.; Owrutsky, J. C. in preparation **2004**.